GEOPHYSICAL RESEARCH LETTERS, VOL. 28, NO. 19, PAGES 3785-3788, OCTOBER 1, 2001

Experimental evidence of inertial waves in a precessing spheroidal cavity

Jérôme Noir, Daniel Brito, Keith Aldridge [1] and Philippe Cardin

Laboratoire de Géophysique Interne et Tectonophysique, Observatoire de Grenoble, France

Abstract. We have demonstrated experimentally the existence of inertial waves in a slowly precessing spheroid of fluid. Although such oscillatory internal shear layers have been predicted theoretically and numerically, previous precession experiments had shown no evidence of their presence. Using an ultrasonic Doppler velocimetry technique, profiles of radial velocity have been measured in our precession experiment. Comparison of these profiles with their synthetic counterparts obtained numerically, proves the presence of the predicted internal shear layers. They are emitted from the breakdown of the Ekman layer at the two critical latitudes of the fluid (around 30° and -30°) and propagate through the entire volume on conical surfaces. The asymptotic laws for these oscillatory layers, confirmed experimentally and numerically, lead us to predict an oscillatory flow of 10^{-6} m/s along such characteristic cones in the Earth's fluid outer core.

Introduction

The Earth's outer core is a conducting liquid with its dynamics significantly determined by the fact that it is a rapidly rotating fluid, contained in a quasi-spheroidal, relatively rigid mantle. While modelling the real Earth's core, complete with its solid inner part, will introduce complexities into its dynamical response to external perturbations, it is important to understand the core's most basic hydrodynamical behaviour first. The laboratory evidence of inertial waves in a precessing spheroid reported here is just such a fundamental property of a contained, rotating fluid.

A primary result in the theory of rotating, barotropic fluids is the existence of characteristic surfaces (cones) along which small disturbances may propagate [*Greenspan*, 1968]. Oscillatory shear layers will develop along conical directions in a contained rotating fluid, when the boundary is perturbed. More specifically, critical latitudes exist on the sphere (and more generally on a spheroid) where the boundary layers thicken significantly [*Stewartson and Roberts*, 1963]. In the experiment described below, the boundary of the container is slowly precessed as seen by an observer rotating with the fluid. The critical latitudes attached to the fluid then become the source of conical shear layers which penetrate the fluid interior [*Kerswell*, 1995]. Following *Greenspan* [1968], these oblique shear layers are identified as an inertial wave.

[1] On sabbatical leave from York University, Toronto, Canada.

Paper number 2001GL012956.
0094-8276/01/2001GL012956$05.00

While our technique of measurement of the fluid velocity (Doppler ultrasonic method) clearly shows the internal shear layers in the precession experiments, observations of reflected light in this experiment and earlier versions of it using both flakes [*Malkus*, 1968] and dyes [*Vanyo et al.*, 1995; *Vanyo and Dunn*, 2000], did not reveal them. Indeed, in only two related experiments concerned mainly with inertial modes [*Greenspan*, 1968; *McEwan*, 1970], were the characteristic cones observed (for a review on inertial modes, see [*Aldridge*, 1997])

The precession experiment

We use a spheroidal cavity whose dimensions are given in Figure 1; its oblateness is $\eta = (a - c)/a = 1/25$. The Doppler measurements were obtained with a rotation rate of the container $\omega_c = 212 \pm 0.02$ rpm imposed by a brushless motor. With water as the working fluid (kinematic viscosity, $\nu \simeq 1.1\ 10^{-6}$ m^2/s) and the above experimental parameters, the Ekman number is $E = \nu/\omega_c a^2 \simeq 3.17\ 10^{-6}$. The container is put on a rotating table which imposes a retrograde precession rate $\vec{\Omega_p}$ varying from 0.1 to 10 rpm while the axis of rotation of the container itself $\vec{\omega_c}$ makes an angle $\alpha = 20^\circ$ with $\vec{\Omega_p}$ (see [*Noir*, 2000] for details).

In *Noir* [2000], flakes (Kalliroscope) have been used to visualise the flow. For example in Figure 2, some parts of the flow were observed using that technique: the illuminated parts of the picture correspond to coherent orientation of the flakes associated with an axisymmetric shear. We note the central brightness around the fluid axis of rotation which is tilted from the axis of rotation of the container $\vec{\omega_c}$, as predicted by linear theory [*Busse*, 1968] and measured through different techniques [*Vanyo et al.*, 1995; *Noir*, 2000]. The bright bands on both side of the photograph are associated with geostrophic motions first measured in *Malkus* [1968]. They are explained by a nonlinear process in the singularity of the boundary layer at critical latitudes. Here, as expected, we have no evidence of oblique shear layers with this visualisation technique.

A Doppler velocimetry method was used to measure the velocity field associated with the inertial wave. This method is based on the shift in frequency of ultrasonic pulses reflected by moving particles (here, conifer pollen spores that are neutrally buoyant) in the fluid. Calibration and validation of this Doppler method have been performed in *Brito et al.* [2001] through quantitative tests. The ultrasonic probe fixed in the precessing frame, points towards the center of the spheroid as shown in Figure 1. This configuration enables us to measure radial velocity along the ultrasonic beam.

Such measurements for different angular velocities of the precessing table are reported in Figure 3. Each experimen-

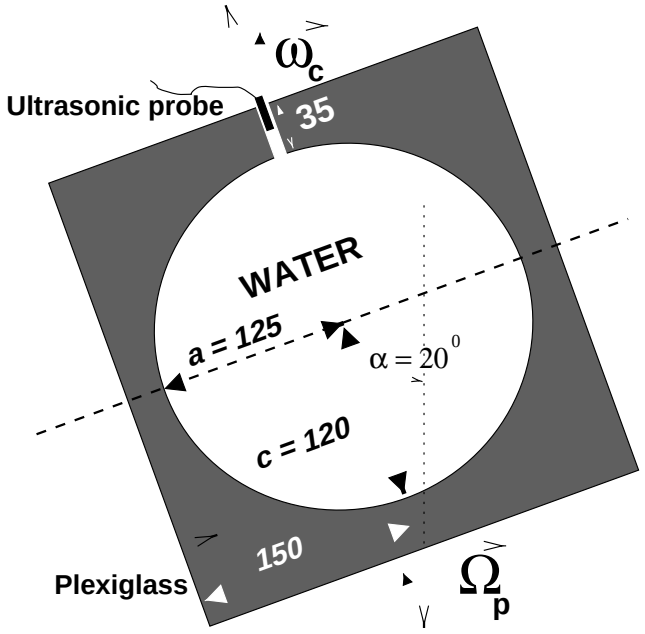

Figure 1. The spheroidal cavity is cut in a plexiglass cylinder (shaded area). Dimensions are in mm. An ultrasonic probe of diameter 8 mm is introduced without contact in the upper hole (10 mm in diameter) of the spheroid.

tal curve (solid line) is the average of 1000 profiles of radial velocity done every 25 ms. Note that the position of the probe in the upper hole has been chosen to minimise the measured velocity at the center of the spheroid for $\Omega_p = -3$ rpm and remained the same for the other precessing rates. Note also that the spatial resolution is better than 3 mm in radius, and the divergence of the beam is 5° corresponding to a lateral resolution increasing from 5 mm to 25 mm along the shooting direction. The combination of these three phenomena produce the error bars shown in Figure 3.

The velocities measured in Figure 3 are stationary in time. Clearly evident is a spatial oscillation along a diameter of the spheroid, with velocities nearly antisymmetric with respect to the center of the spheroid. Should we associate these features with the predicted inertial wave?

Numerical model of precession

We used the numerical model developed in *Noir et al.* [2001] to compute the expected flow in the laboratory experiment. Briefly, this model solves the momentum equation for an incompressible fluid of viscosity ν enclosed in a spherical container of radius R. The sphere is spinning with a frequency ω_c around $\vec{k_c}$, and precessing at Ω_p around $\vec{k_p}$. Units of length and time are chosen as R and ω_c^{-1} respectively. We write the momentum equation in a reference frame attached to the solid-body rotation $\vec{\omega} \times \vec{r}$ of the fluid precessing at Ω_p. Including the centrifugal force in the reduced pressure φ, the momentum equation for $\vec{u}$ is written:

$$\frac{\partial \vec{u}}{\partial t} + 2(P\vec{k_p} + \vec{\omega}) \times \vec{u} + (P\vec{k_p} \times \vec{\omega}) \times \vec{r} + (\vec{u} \cdot \vec{\nabla})\vec{u} = -\vec{\nabla}\varphi + E\vec{\nabla}^2\vec{u}\,,$$

where P is the Poincaré number defined as Ω_p/ω_c. No-slip and no-penetration boundary conditions are used at r=1.

Figure 4 shows the three components of velocity in the plane $(\vec{\omega}, \vec{k_c})$ in the frame attached to the solid-body rotation of the fluid for $E = 3.16\ 10^{-6}$ and $P = -1.8\ 10^{-4}$. For this low value of the Poincaré number, geostrophic motions are very weak and cannot be seen in the figure.

In *Noir et al.* [2001], it is shown that the amplitude of the inertial wave scales as $\epsilon E^{1/5}$ where $\epsilon = |\vec{\omega} - \vec{k_c}|$ is the forcing associated with differential rotation between the fluid and the boundary. In the range of parameters of our experiment, it can also be shown that ϵ is proportional to $\sin\beta$ where β is the angle between $\vec{\omega}$ and $\vec{k_c}$ [*Busse*, 1968].

For the Ekman number of the computation shown in Figure 4, the size (or wavelength) of the inertial wave which scales as $E^{1/5}$ [*Kerswell*, 1995] is large ($\approx R/3$) and asymptotic features, such as characteristic cones, are difficult to appreciate. Lower values of the Ekman number clearly show this asymptotic behavior (see [*Noir et al.*, 2001]). Oscillating shear layers emerge around critical latitudes at $\theta = \pm 30°$ with respect to the axis of rotation of the fluid. We see the singularity of the Ekman layer at that latitude in the u_θ, u_ϕ velocity contours in Figure 4, which generates a radial flow in and out from this region. The shear propagates inside the fluid along characteristic conical surfaces, symmetric about the axis of rotation of the fluid with a semi-angle of 30°. These inertial waves are time dependent with a pulsation ω in the frame attached to the solid-body rotation of the fluid. They are stationary in the precessing frame, in particular on the axis of rotation of the spheroid $\vec{k_c}$ where the ultrasonic experimental probe is attached.

Comparison

The source of the inertial wave is a local phenomenon: the ellipticity of the container is not crucial as long as the oblateness η is small compared to the size of the eruption of the boundary layer ($E^{1/5}$). Since this condition is met

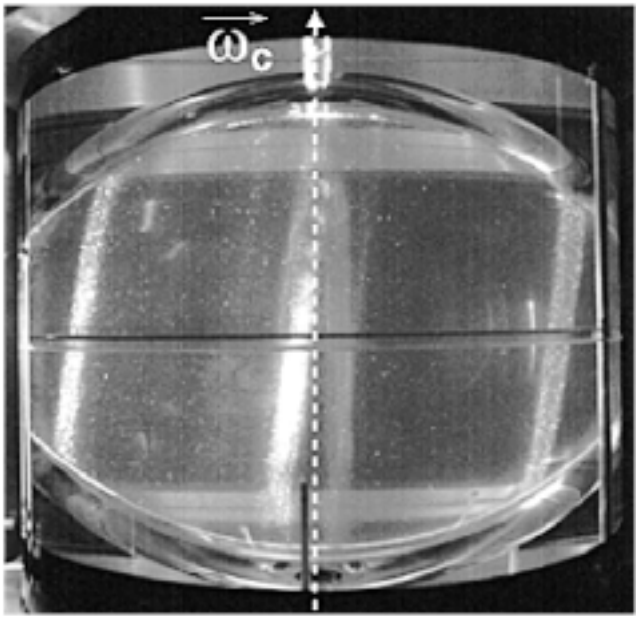

Figure 2. Photograph of flakes in the spheroidal cavity for $\alpha = 20°$, $\omega_c = 300$ rpm and $\Omega_p = -3$ rpm. Bright bands show the shear associated with both the axis of rotation of the fluid and geostrophic motions.

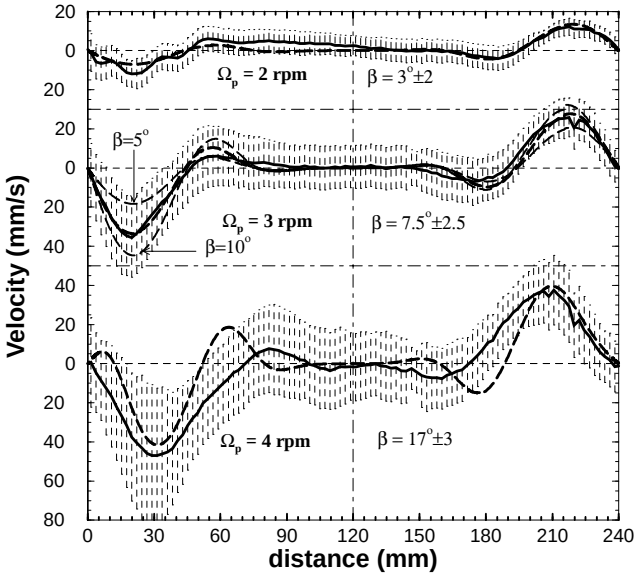

Figure 3. Measured profiles of radial velocity (solid lines) obtained from Doppler ultrasonic velocimetry for $\alpha = 20°$, $\omega_c = 212$ rpm and three precessing rates Ω_p. The vertical bars give the standard deviation of velocity. Dashed lines are numerical velocity profiles deduced from figure 4 with the best value of the colatitude β fitting the data. In order to illustrate the sensitivity of this method, extreme numerical profiles contained within error bars ($\beta = 5^o$,$\beta = 10^o$) are shown for $\Omega_p = -3$ rpm.

in the present experiment, we can compare the numerical calculations (from the spherical model) with the experimental data measured in the spheroidal container. For larger ellipticity ($> E^{1/5}$), spheroidal models should be used as in *Lorenzani and Tilgner* [2001].

First, we consider only the inertial wave component part of the flow in Figure 4 (ϕ wavenumber m=1). Second, let us consider a colatitude angle β with respect to the axis of rotation of the fluid $\vec{\omega}$ (vertical axis in Figure 4): along this angle, we can extract a profile of radial velocity. Note that a change in β will change the shape of the profile. Third, in order to obtain the amplitude of the synthetic profile for a given colatitude β, we use the asymptotic scaling $\sin\beta E^{1/5}$ as proposed in the previous section. We have therefore $A(r)/A^*(r) = \sin\beta/\sin\beta^*$ where A denotes the amplitude of the synthetic inertial wave and the star stands for the numerical calculation. The calculation in Figure 4 gives $\sin\beta^* = 0.016$. Note that we have neglected the Ekman number dependency in the relation given above as the two Ekman numbers are equal. The last step is then to find the colatitude β which best explains the experimental data in shape and in amplitude using a least squares method, and compare it with independent estimations of β.

As seen in Figure 3 where we have represented both the experimental and numerical profiles, we find $\beta = 3°,\ 7.5°,\ 17°$ for $\Omega_p = -2,\ -3,\ -4$ rpm respectively. We compare these determinations of β both to their evaluations in the experiments through visualization and pressure measurements which give $7° \pm 5°$, $11° \pm 5°$ and $20° \pm 5°$ respectively, and to the asymptotic results [*Busse*, 1968] which give 5.6°, 9.8° and 17° respectively.

Note that the asymmetry between the first and second half of each profile in Figure 3 is explained by the divergence of the ultrasonic beam mentioned earlier. The numerical profiles reproduce this asymmetry when averaging over a sampling volume that increases along the diameter.

The agreement between experimental and numerical profiles demonstrates unambiguously that the spheroidal precessing container induces oblique internal shear layers in the fluid. Figure 3 also checks experimentally the asymptotic scaling laws for the amplitude of the velocity $\epsilon E^{1/5}$ and the size $E^{1/5}$ of this inertial wave. An experimental verification of the Ekman number dependency of the scaling laws needs experiments at different ω_c, although it will be difficult to check the 1/5 exponent with the decade in Ekman numbers accessible experimentally here. Finally, this study shows that it is legitimate to compare a spherical numerical calculation with our spheroidal experimental work, regarding local phenomena such as these oblique or geostrophic shear layers (see [*Noir et al.*, 2001]).

Discussion

Why do flakes not see inertial waves?

There is no evidence of conical features with the flakes technique, even though we know that this technique is very sensitive to velocity shear. The flakes need a transient time

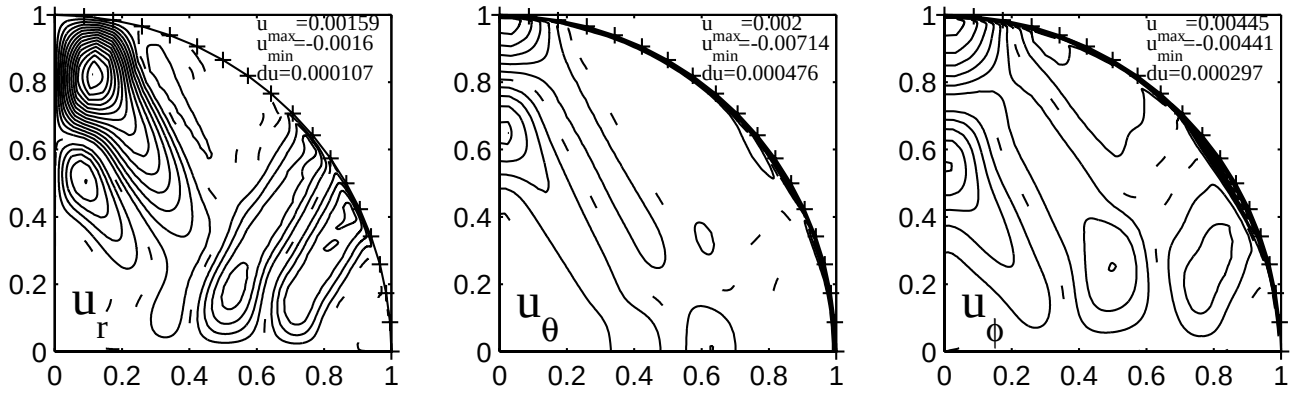

Figure 4. The three spherical components u_r, u_θ, u_ϕ of the precessing flow in a sphere in the meridional plane containing $\vec{k_c}$ and $\vec{\omega}$. $E = 3.16\ 10^{-6}$ and $P = -1.8\ 10^{-4}$. Contour intervals du, maxima and minima are indicated on each figure. Solid (dashed) lines: positive (negative) values. Dotted line: zero isocontour line.

to align in the shear, which one can estimate as the inverse of the shear rates. Using figure 3, the maximum shear rate is $(\Delta u/\Delta d)_{max} \simeq (50\ mm/s)/(30\ mm)$ which gives a transient time equal to at least 0.6 s. Since the period of the inertial wave is 0.28 s, it seems reasonable to conclude that flakes have no time to line up in the internal shear layers.

Application to the Earth's Core

Both the numerical studies and the present experimental work enable us to propose the law $1.5\ \epsilon\ E^{1/5}\ R\ \omega_c$ (in dimensional units) for the maximum amplitude of the radial velocity of the inertial wave induced by the precession of the outer boundary of a spheroid. Using $\epsilon = 1.7\ 10^{-5}$ and $E = 10^{-15}$, we find that the inertial wave in the outer core associated with the precession of the Earth corresponds to a diurnal oscillation of the fluid of amplitude $6\ 10^{-6}$ m/s on a width of 20 km (*e.g.* a displacement of 0.2 m in 12 hours). This is smaller than 10^{-4} m/s which is a typical fluid velocity at the top of the Earth's Core deduced from secular variation of the Earth's magnetic field [*Bloxham and Jackson*, 1991]. If we ignore both the action of the magnetic field and possible destabilisation of this flow (turbulence, viscous or elliptical instabilities, ...), these values could be used for direct prediction of motions in the Earth's core excited by the luni-solar precession.

Acknowledgments. Financial support for the experimental set-up came from the Région Rhône-Alpes and CNRS/INSU. We wish to thank the University Joseph Fourier for inviting Prof. K. Aldridge and also thank H.C. Nataf, D. Jault and J.P. Masson for useful discussions.

References

Aldridge, K. D., Perspectives on Cores Dynamics from Laboratory Experiments, in *Earth's Deep Interior*, edited by D. J. Crossley, pp. 65-78, 1997.

Bloxham, J., and A. Jackson, Fluid flow near the surface of Earth's outer core, *Rev. Geophys., 29,* 97-120, 1991.

Brito, D., H.-C. Nataf, P. Cardin, J. Aubert, and J.-P. Masson, Ultrasonic Doppler velocimetry in liquid gallium, in press in *Exp. Fluids*, 2001.

Busse, F. H., Steady fluid flow in a precessing spheroidal shell, *J. Fluid Mech., 33,* 739-751, 1968.

Greenspan, H. P. *The theory of rotating fluids,* 325 pp., Cambridge University Press, U.K., 1968.

Kerswell, R. R., On the internal shear layers spawned by the critical regions in oscillatory Ekman boundary layers, *J. Fluid Mech., 298,* 311-325, 1995.

Lorenzani, S., and A. Tilgner, Fluid instabilities in precessing spheroidal cavities, *J. Fluid Mech., submitted,* 2001.

McEwan, A. D., Inertial oscillations in a rotating fluid cylinder, *J. Fluid Mech., 40,* 603-640, 1970.

Malkus, W. V. R., Precession of the Earth as the Cause of Geomagnetism, *Science, 160,* 259-264, 1968.

Noir, J., Écoulements d'un fluide dans une cavité en précession. Ph. D. thesis, 163pp., Université Grenoble 1, France, November 2000.

Noir, J., D. Jault, and P. Cardin, Numerical study of the motions within a precessing sphere, at low Ekman number, *J. Fluid Mech., 437,* 283-299, 2001.

Stewartson, K., and P. H. Roberts, On the motion of a liquid in a spheroidal cavity of a precessing rigid body, *J. Fluid Mech., 17,* 1-20, 1963.

Vanyo, J., P. Wilde, P. Cardin, and P. Olson, Experiments on precessing flows in the Earth's liquid core, *Geophys. J. Int. 121,* 136-142, 1995.

Vanyo, J. P., and J. R. Dunn, Core precession: flow structures and energy, *Geophys. J. Int. 142,* 409-425, 2000.

J. Noir, D. Brito and P. Cardin, LGIT, Université Joseph Fourier, CNRS, BP 53, 38000 Grenoble, France. (e-mail: philippe.cardin@ujf-grenoble.fr)

K. Aldridge, Centre for Research in Earth and Space Science, York University, 4700 Keele Street, Toronto, Ontario, M3J 1P3, Canada. (e-mail: keith@yorku.ca)

(Received February 5, 2001; revised May 17, 2001;
accepted June 25, 2001.)